A Solid-State Metal Hydride/Oxygen Cell using $La_{0.78}Ce_{0.22}Ni_{3.73}Mn_{0.30}Al_{0.17}Fe_{0.50}Co_{0.30}$in the Anodeand Nafion as Electrolyte

Yu-Bin ZHANG[1,a,*], Chao-Ling WU[1,2,b,*],Yun-Gui CHEN[1, 2], Li-Wu HUANG[1], Ding ZHU[2], XuDAI[1]and Wan-Hai ZHOU[1]

[1]Department of Advanced Energy Materials, College of Materials Science and Engineering, Sichuan University, Chengdu 610064, China

[2]Institute of New Energy and Low-Carbon Technology, Sichuan University, Chengdu 610064, China

[a]email address: zhangyubin.ok@163.com

[b]email address: wuchaoling@scu.edu.cn

Keywords: Metal hydride/Oxygen cell,Solid electrolyte,Nafion,Electrochemical properties

Abstract. A solid polymer electrolyte metal hydride (MH)/oxygen cell using $La_{0.78}Ce_{0.22}Ni_{3.73}Mn_{0.30}Al_{0.17}Fe_{0.50}Co_{0.30}$in the anode and Nafion as electrolyte is described and investigated experimentally. In this work, the discharge performances of the cell are compared in two charging ways, namely, electrochemical and gas-solid hydrogenation. The specific discharge capacityby gas-solid hydrogenation method is about 59.3mAh·g^{-1}, while almost few specific discharge capacityis obtained by electrochemical method in this work. The cell is characterized by means of X-ray diffraction (XRD) and scanning electron microscopy (SEM) analyses. And the ex-situ XRD results of the cell charged by gas-solid hydrogenation method show that an electrochemical reaction between hydrogen and oxygen does happen, and little observable side reaction occurs. Moreover, the stability of the MH electrode depending on various relative humidity is investigated. The results indicate that solid-state MH/O_2 cell using Nafion as electrolyte is technically feasible, while the control of the water content during charge/discharge processes and the catalyst loading must be the key points. More than that, further researches are still required to enhance both charge/discharge capacity and reversibility.

Introduction

Nickel/metal hydride (Ni/MH) battery has been received many interests since 1990s because of its excellent electrochemical characteristics, long cycle life and environmental friendliness[1-3].In Ni/MH battery, the specific charge/discharge capacity is limited by Ni electrode[4].So in order to improve the specific capacity of the battery, it is necessary to replace the heavy Ni electrode with a lightweight electrode, for example air electrode.

Besides, in ordinary MH/O_2battery, a KOH aqueous solution is currently used as an electrolyte. And the corrosion of air electrodes made of catalyzed carbon materials [4],the neutralization of KOH with CO_2[5]and the corrosion of some family of hydrogen storage alloys still remain. In order to solve these problems, a solid polymer electrolyte is considered to replace the conventional KOH electrolyte [6].The battery with solid polymer electrolytes normally has some advantages such as reliability, safety and ease of cell designing compared with those using the conventional liquid electrolyte[7].And in 2013, Andrew J.[8] has proposed and investigated proton flow battery which is similar to MH/O_2using Nafion as the electrolyte. Their work focus on the contrast between the new system and the conventional hydrogen cycle including hydrogen production by electrolysis, hydrogen storage and application.

Inspired by their study, in our work, we introduce Nafionmembraneas solid polymer electrolyte in MH/O_2 cell. And because of the highly reversible hydrogen sorption, low equilibrium pressure and the relatively fast kinetics [9]of AB_5series, the commercialized hydrogen storage alloy

$La_{0.78}Ce_{0.22}Ni_{3.73}Mn_{0.30}Al_{0.17}Fe_{0.50}Co_{0.30}$ was used. Different charge methods namely electrochemical and gas-solid hydrogenation and the processes of the charge/discharge were investigated.

MH/O_2Cell Chemistry

The charge/discharge reactions for the MH/air rechargeable battery using an air electrode as the cathode, $La_{0.78}Ce_{0.22}Ni_{3.73}Mn_{0.30}Al_{0.17}Fe_{0.50}Co_{0.30}$(M)as the anode and Nafion as the electrolyte solution proceed as follows:

- At the positive electrode:

$$2H_2O \underset{discharge}{\overset{charge}{\rightleftharpoons}} 4H^+ + O_2 \uparrow +4e \tag{1}$$

- At the negative electrode:

$$XH^+ + Xe + M \underset{discharge}{\overset{charge}{\rightleftharpoons}} MH_X \tag{2}$$

- Overall reaction:

$$\frac{4}{x}M + 2H_2O \underset{discharge}{\overset{charge}{\rightleftharpoons}} \frac{4}{x}MH_x + O_2 \uparrow \tag{3}$$

During the charge process, oxygen gas is produced by water electrolysis on the air electrode and during the discharge process oxygen gas must be supplied to the air electrode[10].

The Advantages of the New Type MH/O_2System

In comparison with the conventional MH/O_2, the new MH/O_2 system has the merits of reduction of the electrode corrosion, improvement of the battery life, elimination of the problems of battery leakage, reliability, safety and ease of cell designing.

The new type MH/O_2 system not only takes the advantages of conventional fuel cell, which are high-efficiency, less-emission,[11, 12] but also obtains a compact and simple structure with a high energy density and increases roundtrip efficiency by eliminating the intermediate steps of hydrogen gas production, storage and recovery. Meanwhile, it overcomes the unneglectable difficulties during hydrogen production, distribution and storage.[8, 13, 14]

Compared with the Metal/O_2 battery such as Zn/O_2 or Fe/O_2battery, the innovative MH/air system deems to exhibit a relatively long lifetime and high charging efficiency because of the excellent electrochemical property of hydrogen storage alloys. [4, 15]

Another innovative feature of the MH/air system is that it permits a new battery can be regenerated in two different ways, namely, by gas-solid hydrogenation charging and by electrochemical charging. This allows a more flexible infrastructure for zero emission vehicles.[4, 13]

Experimental

Preparation of the Cell

The processes to fabricate a new type cell were identical to those used in the preparation of membrane electrode assembly (MEA) with catalyst-loaded substrate method.[16]In this research, the commercially available membranes (Nafion 117) with the loading of 4.0mgcm^{-2} bifunctional electrocatalyst Pt/Ir (50:50) as oxygen electrode were obtained from HesenCorporation. Then, to make the MH electrode, 0.153g $La_{0.78}Ce_{0.22}Ni_{3.73}Mn_{0.30}Al_{0.17}Fe_{0.50}Co_{0.30}$ powder, whose D10% is6.065μm, D50%21.310μm, D90%46.791μm, and the average size is 24.620μm,was added into the mixture of 1.125ml Nafion solution (Nafion,D-521,Dupont) and 0.021g acetylene black, which was

stood statically at room temperature for 1h. Then supernatant liquid was dried at 25℃ in a vacuum for 15min, and the slurry was brushed onto a carbon paper substrate as a collector and dried at 25°C for 30min in a vacuum oven. The hydrogen storage alloy loading for each electrode was around2.5 $mgcm^{-2}$.

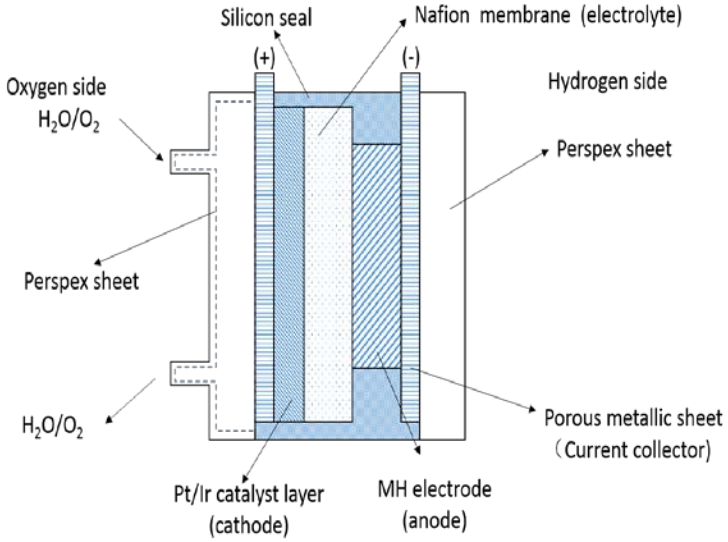

Fig. 1. Schematic design of the $ML(NiCoMnAlFe)_5$ |Nafion $|O_2$ cell.

Finally, the membrane with the Pt/Ircatalysts and the MH electrode in a 2.5*2.5 cm^2active area were bonded together by a hot pressing method, which was conducted at 140 ℃ with a pressure of 10MPa for 90 s. For effective contact between the MH electrode and the polymer electrolyte, the mixture of is opropanol (IPA)/Nafion (0.2ml/0.6ml) solution with the density of 2.0 $mgcm^{-2}$was again brushed on the MH electrode layer. This MEA was obtained and then assembled into a specially-designed stack sealed with a silicone gel. And a schematic of the design of the $La_{0.78}Ce_{0.22}Ni_{3.73}Mn_{0.30}Al_{0.17}Fe_{0.50}Co_{0.30}$|Nafion $|O_2$ battery is shown in Fig. 1.

Cell Characterization

X-ray diffraction (XRD) was recorded by DX-2600 X-ray diffractometer using Copper K α radiation source (l=0.15406nm) at 35kV and 25 mA with 2θ from 20° to 80° and step span of 0.03° .

The cross-sectional morphologies of MEA was investigated by using scanning electron microscopy (SEM,JSM-6460,JEOL,Tokyo,Japan).

All the experiments were carried out at room temperature.

Electrochemical Measurement

In charge mode, the cells using electrochemical method were charged at a current density of 0.08 mA cm^{-2}under Land CT2001A battery-testing system. While the cells by gas-solid hydrogenation method were charged directly by an automated Sievert's apparatus(PCTPro-2000 from Hy-Energy LLC).The hydrogenated MEA were obtained under 40 bar and 40°C.

In discharge mode, the galvanostatic discharge tests were carried out at a current density of 0.008 $mAcm^{-2}$from an open-circuit voltage (OCV) to 0V under Land CT2001A battery-testing system. In this mode, variations of voltage over time were recorded.

All the electrochemical experiments were carried out after 12h of the assembly of the cells in order to make the silicone gel dry.

Results and Discussion

Structure and Morphology Characterization of MEA

The XRD patterns of the anodeside of MEA are obtained in Fig.2.As shown in Fig.2, except for the extra peaksascribed to carbon (PDF: 41-1487), all peaks can be indexed by a single hexagonal $CaCu_5$-type $LaNi_5$ phase. Besides， the lattice contents and the cell volume of the hydrogen storage alloy are that a = 5.028Å, c=4.046Å and 88.633Å^3,respectively.

Fig.3 shows cross-sectional SEM images of the MEA, in which three layers of anode, Nafionmembrane and cathode are clearly observed. As is seen from Fig.3, good contact in two interfaceis obviously visible which is expected to provide electron and proton channels.

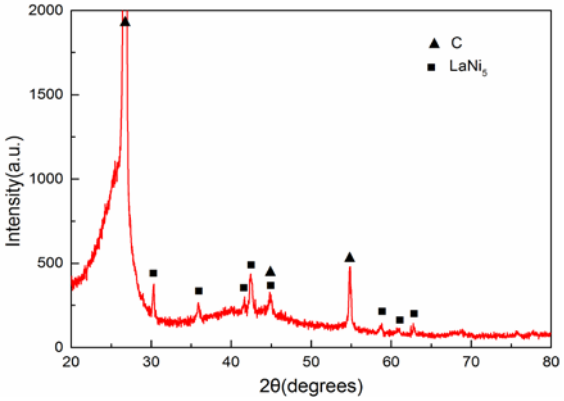

Fig. 2. XRD patterns of the anode side of MEA.

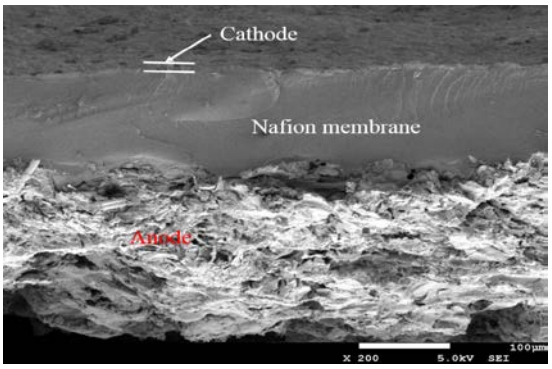

Fig. 3. The cross sectional SEM images of MEA

The electrochemical properties of the cell charged with gas-solid hydrogenation method. The galvanostatic discharge curves the cell charged with gas-solid hydrogenation method at the current density of 0.008 mA cm^{-2}are obtained in Fig.4(a). As can be seen from Fig.4(a), a flat plateau around 0.5V is obtained. And the specific discharge capacity of 59.3mAhg^{-1}is shown, with the estimated hydrogen storage of 0.165wt% in the alloys. And in order to demonstrate the occurrence of the electrochemical reactions, X-ray diffraction analysis was performed.

Fig.4(b) shows the XRD patterns of MEA during discharge process relating to the pointsa~con the voltage curve in Fig.4(a).As indicated in the figure, at the start of the discharge process, except for the extra peaks ascribed to carbon substrates, the other XRD peaks of the initial electrode are assigned to $LaNi_5H_5$.With the proceeding of discharge, new peaks appear which are assigned to $LaNi_5$ phase. And by the end of the discharge process, there is a single $LaNi_5$ phase. All in all, the change of XRD patterns of the discharge sample shows the disappearance of a hydrogenated phase, the presence of a hydrogen storage alloy, and the remaining carbon, which indicates that there is indeed an electrochemical reaction.

Besides, the cycle performance of the MEA was investigated, however, there is almost not any discharge specific capacity of this cell in the 2nd cycle in our work. The reasons need to be further studied.

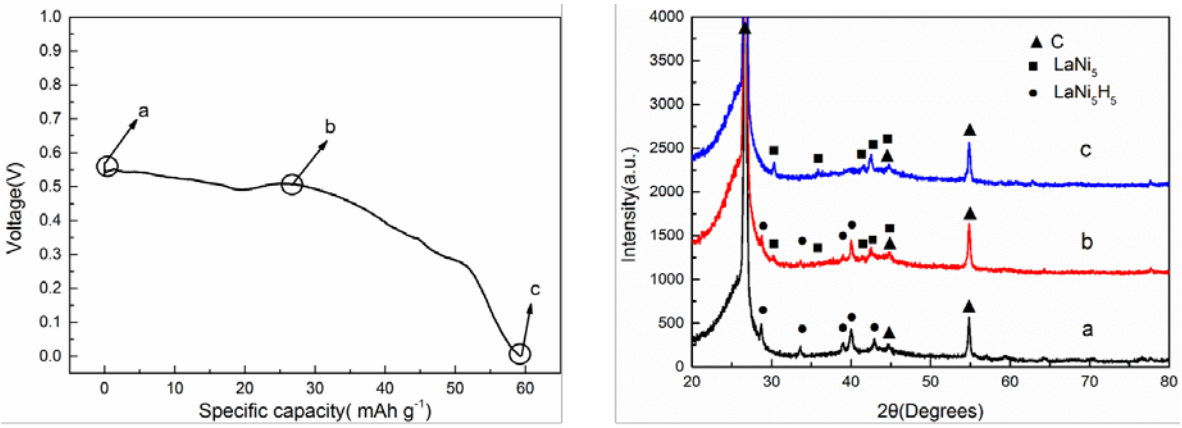

Fig. 4. The galvanostatic discharge curves of MEA charged with a gas-solid hydrogenation method (a), and the corresponding XRD patterns evolution of MEA during the discharge process (b).

The Cell Charged with Electrochemical Method

The charge/discharge tests of the new type cell with electrochemical charge method were conducted. In charge mode, the oxygen electrode was filled with water, while in discharge mode, water was drained from the cell and the oxygen electrode was filled with oxygen at a flow rate of 100 sccm. Typical charge curve is presented in Fig.5, which shows that the voltage reaches to around 1.3V during charge. Unfortunately, however, there is almost not any discharge specific capacity of this cell, which indicates that the hydrogen atoms directly form hydrogen molecules and evolve into the atmosphere instead of entering the electrode and forming MH, and the phenomenon has been proved by the XRD results. As can be seen from Fig.6, the XRD patterns shows there is no new phase after charge/discharge process except for the remaining original hydrogen storage alloy and carbon. In order to analyze the reasons for the poor charge efficiency of the cell, the process of the hydride formation and the stability of the hydride electrode are considered.

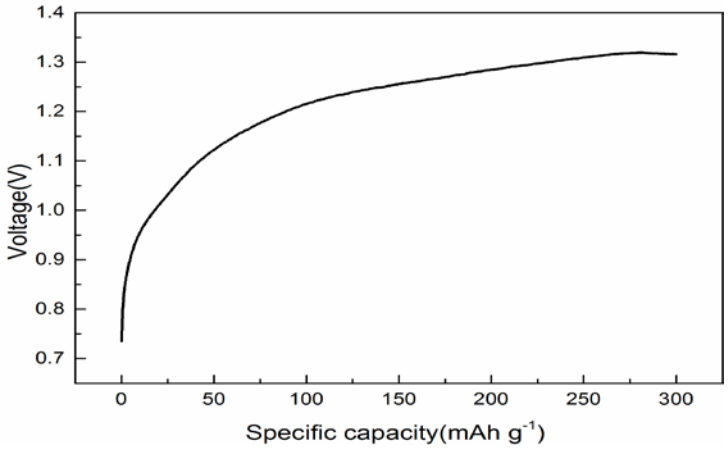

Fig. 5. The galvanostatic charge curve of the cell.

Actually, the hydride formation experiences a series of chemical reactions including interface reaction and mass transport which is similar to the process of Ni/MH battery.[17-20]Firstly, the reactant protons are first supplied by the oxygen evolution reaction on the anode.

$$2H_2O \rightarrow 4H^+ + O_2 + 4e \quad (4)$$

Then, the charge transfer reaction occurs at the interface between the solid polymer electrolyte and the alloy. The reductive atomic hydrogen H(ads) is chemically adsorbed on the surface.

$$H^+ + e + M \rightarrow MH_{ads} \quad (5)$$

Next, the adsorbed hydrogen atoms diffuse into the interior of the alloy powders to become absorbed hydrogen atoms (H_{abs}) and finally proceed to form the metal hydride.

$$MH_{ads} \rightarrow MH_{abs} \quad (6)$$

$$MH_{abs} \rightarrow MH_{hyd} \quad (7)$$

Based upon the knowledge of self-discharge, when MH electrode is stored at open circuit, the hydrogen evolution reaction(HER) is prone to occur due to the relatively low hydrogen evolution over potential.

$$MH_{ads} \rightarrow M + H_{ads}, 2H_{ads} \rightarrow H_2 \uparrow \quad (8)$$

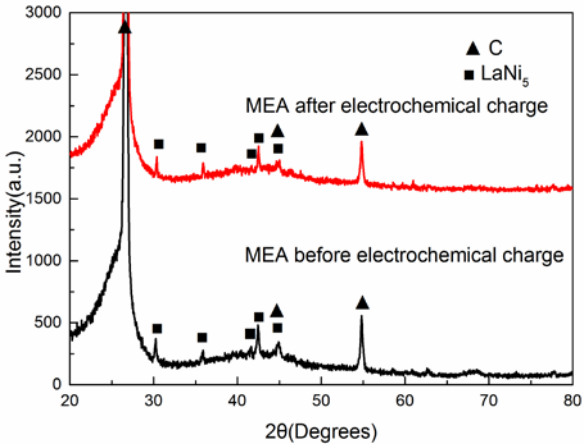

Fig. 6. The XRD patterns of MEA before/after electrochemical charge.

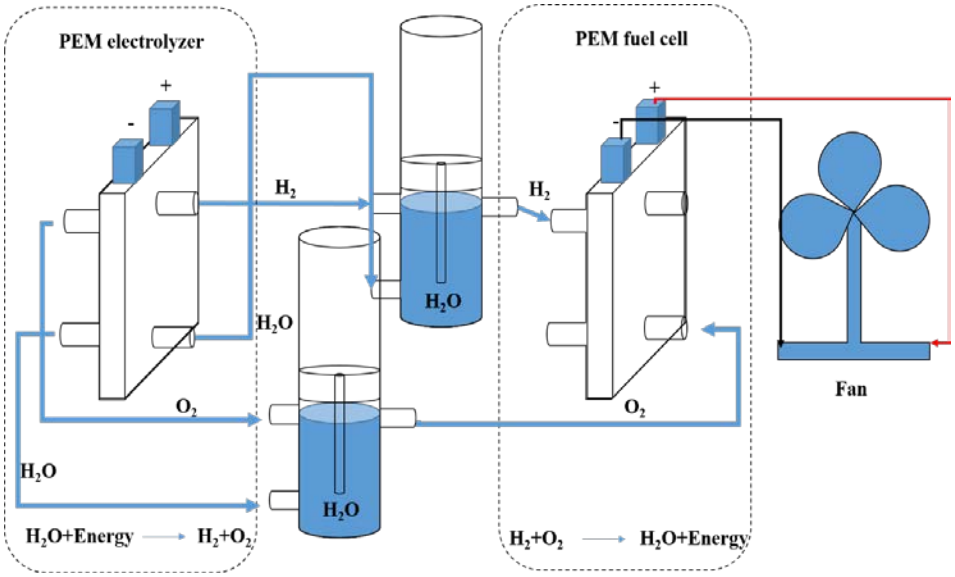

Fig. 7. The schematic process of the verification test.

According to the processes of hydride formation, the possible difficulties of forming the metal hydride may be caused by the barriers of proton production, transmission, the electrochemical

reactionor the diffusion of hydrogen atoms into the alloy powders. The results that there is no difficulty of proton production and transmission through Nafionmembrane had been proved by the experiment using the normal electrolyser with Pt/Ir (1:1,4mgcm^{-2}) as electrocatalysts and Nafion membrane as electrolyte. The schematic process is shown in Fig.7. As shown in Fig.7, the normalelectrolyser as mentioned above converts electric energy into chemical energy in the form of hydrogen and oxygen respectively, and then the produced hydrogen and oxygen were filled in the PEM fuel cell, the chemical energy is directly converted into electric energy through fuel cell to support the fan to work. So, the phenomenon of the rotation of the fan indicates that the normal electrolyser works well which means there is no difficulty of proton production and transmission through Nafion membrane.

Besides, from the results of the higher specific discharge capacity of the new type cell with gas-solid hydrogen uptake method, it is safely concluded that the Nafionand acetylene black have formed an efficient three dimensional conductive framework. And because of the charging current density is low enough, the diffusion of hydrogen atoms into the alloy powders is not the main problem[17-20].So, excluding the above reasons, the interruption of the electrochemical reaction may be one of the reasons contributing to the difficulty of charging. In order to solve this problem, the addition of electrocatalysts such as nickel needs to be considered. And further research is still required.

On the other hand, thecombination of fluorinated backbone and sulfonic acid groups makes Nafion a very strong acid[21, 22]. So the stability of the hydride electrode at different humidity needs to be further discussed.

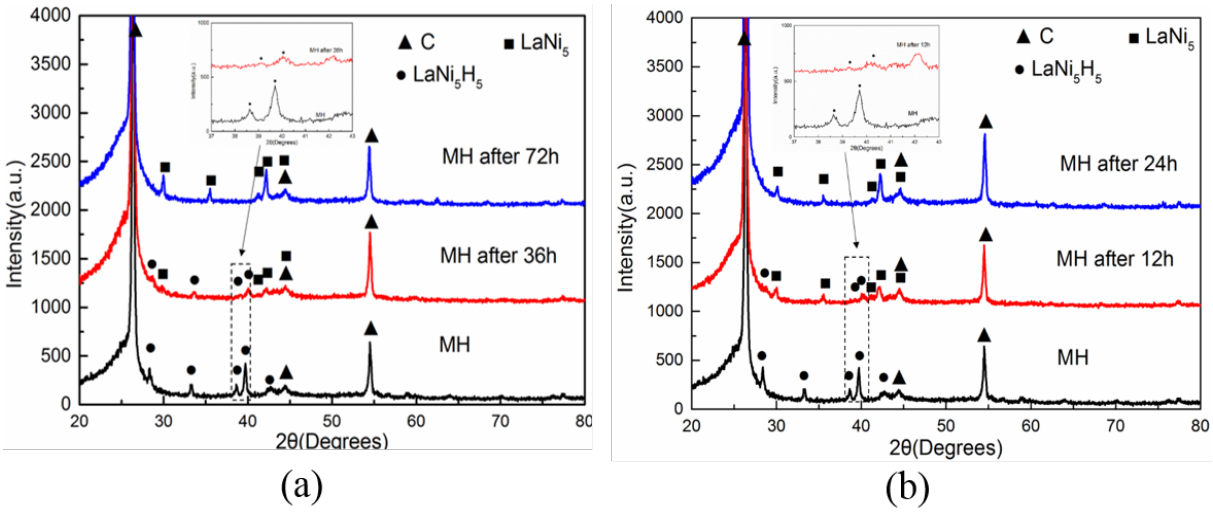

Fig. 8. The XRD pattern evolution of the MEA during the standing process respectively at the relatively humidity of 60% (a) and 100% (b).

In order to study the stability of the hydride in acid Nafion, MH in the relative humidity of 60% and 100% were investigated, respectively. The change of XRD patterns of MH with the increasing of standing time at different conditions is obtained in Fig. 8.As seen in Fig.8(a), after 36h, at the relative humidity of 60%,the XRD patterns of MH shows the presence of a hydrogen storage alloy phase, and the peaks of $LaNi_5H_5$shift slightly to higher degrees, which implies that hydrogen atoms Evolved from the interstitial sites in the lattice of the hydrogen storage alloys. And up to 72h, there is only a single $LaNi_5$ phase. Fig.8(b) shows a similar variation at relative humidity of 100%. But the starting time of the change is obviously shortened, and in order to analyze the reason of the results, the microstructure of Nafion is discussed. According to the previous studies of Nafion[22-24], the Small Angle X-ray Scattering (SAXS) patterns shows an increase in the intensity of the ionomer peak and a shift to lower scattering angle with the increase of the relative humidity which suggests the number and size of the clusters increased with increasing relative humidity. And the corresponding maximum entropy (MaxEnt) electron density maps of Nafionalso showsan overall increase in electron density associated with an increase in water uptake. And the

results indicate the increase of the number of clusters. Based on the basic cluster-network model of earlier investigation, the increase of the number of sulfonate ion clusters means there are more corresponding equilibrium H_3O^+ which may attribute to the increase of contact opportunity between H_3O^+ and the hydrogenated alloys. And according to previous researches, thehydride is unstable in acid case which means that the hydrogen atom will evolve from the hydrogenated alloys. So, more contact possibility between the H_3O^+ and the hydrogenated alloys maybe the reason of the shorter change time of the hydrogenated phase with the increase of relative humidity.So,the control of the water content during both charge and discharge processes must be one of the key points.

Though the performances of the MH/O_2 battery using Nafion as electrolyte with electrochemical and gas-solid hydrogenation method in our study are poor, more studies such as using graphene which can provide both proton and electron channels[25]or preparing the protection layer for hydrogen storage alloys need to be done to solve the problem of the unstability of the hydrogenated anode. Besides, the addition of electrocatalysts such as nickel helps to form the hydrogenated electrode in the electrochemical method. Apart from these, other families of hydrogen storage alloys with higher theoretical energy density such as Mg-based hydrogen storage alloys (MgH_2:1900 Wh/kg), which has been shown to be seriously corroded in alkaline solution, can be a potential candidate for use as an anode material in the innovative MH/O_2 battery.

Conclusions

In this paper, a solid polymer electrolyte metal hydride (MH)/oxygen cell using Nafion as electrolyte is fabricated and investigated experimentally. And the charge/discharge performances of the cell are compared in two charging ways, namely, electrochemical and gas-solid hydrogenation. As for the cell charged by gas-solid hydrogenation, the specific discharge capacity of 59.3mAh g^{-1} is obtained under the current density of 0.008 mA cm^{-2}, with the estimated hydrogen storage of 0.165wt% in the $La_{0.78}Ce_{0.22}Ni_{3.73}Mn_{0.30}Al_{0.17}Fe_{0.50}Co_{0.30}$ alloys. And the corresponding ex-situ XRD results indicate that there is indeed an electrochemical reaction. While for the cell charged by electrochemical method, there is few specific discharge capacity observed, which indicates that the hydrogen atoms directly form hydrogen molecules and evolve. One of the possible reasons may be the interruption of the electrochemical reaction during hydride forming process which needs to be further studied. Besides, the research results of the stability of MH at different relative humidity show that with the increase of the standing time, the hydrogen atoms will evolve from MH automatically. So, the control of the water content during both charge and discharge processes must be one of the key points.

References

[1] T. Sakai, I. Uehara, H. Ishikawa, J. Alloys Compd, 293–295 (1999) 762-769.

[2] F. Feng, M. Geng, D.O. Northwood, Int. J. Hydrogen Energy 26 (2001) 725-734.

[3] A.K. Shukla, S. Venugopalan, B. Hariprakash, J. Power Sources 100 (2001) 125-148.

[4] T. Sakai, T. Iwaki, Z. Ye, D. Noreus, J. Electrochem. Soc. 142 (1995) 4040-4045.

[5] N. Fujiwara, M. Yao, Z. Siroma, H. Senoh, T. Ioroi, K. Yasuda, J. Power Sources 196 (2011) 808-813.

[6] N. Vassal, E. Salmon, J.-F. Fauvarque, J. Electrochem. Soc. 146 (1999) 20-26.

[7] K. Hatakeyama, H. Sakaguchi, K. Ogawa, H. Inoue, C. Iwakura, T. Esaka, J. Power Sources 124 (2003) 559-563.

[8] J. Andrews, S. Seif Mohammadi, Int. J. Hydrogen Energy 39 (2014) 1740-1751.

[9] H. Falahati, D.P.J. Barz, Int. J. Hydrogen Energy 38 (2013) 8838-8851.

[10] A.A. Mohamad, N.S. Mohamed, Y. Alias, A.K. Arof, J. Power Sources 115 (2003) 161-166.

[11] M.R. von Spakovsky, B. Olsommer, Energ. Convers. Manage. 43 (2002) 1249-1257.

[12] O.Z. Sharaf, M.F. Orhan, Renew. Sust. Energ. Rev. 32 (2014) 810-853.

[13] C. Folonari, G. Iemmi, F. Manfredi, A. Rolle, J. Less-Common Met. 74 (1980) 371-378.

[14] W. Chaoling, C. Yungui, H. Zhifen, W. Qiang, Y. Fei, W. Haiwen, W. Xiaolian, in: Proceedings of 2011 China Functional Materials Technology and Industry Forum, China Academic Journal Electronic Publishing House, Chongqing, China(2011), pp. 934-942.

[15] F.R. McLarnon, E.J. Cairns, J. Electrochem. Soc. 138 (1991) 645-656.

[16] S. Thanasilp, M. Hunsom, Fuel, 89 (2010) 3847-3852.

[17] L. Yongfeng, P. Hongge, G. Mingxia, W. Qidong, J. Mater. Chem. 21 (2011) 4743-4755.

[18] B. Hariprakash, A.K. Shukla, S. Venugoplan, Secondary Batteries – Nickel Systems | Nickel–Metal Hydride: Overview, in: J. Garche (Ed.) Encyclopedia of Electrochemical Power Sources, Elsevier, Amsterdam, 2009, pp. 494-501.

[19] B. Sakintuna, F. Lamari-Darkrim, M. Hirscher, Int. J. Hydrogen Energy 32 (2007) 1121-1140.

[20] M. Geng, D.O. Northwood, Int. J. Hydrogen Energy 28 (2003) 633-636.

[21] K.D. Kreuer, M. Ise, A. Fuchs, J. Maier, J. Phys. IV 10 (2000) 279-281.

[22] K.A. Mauritz, R.B. Moore, Chem. Rev. 104 (2004) 4535-4585.

[23] J. Halim, G.G. Scherer, M. Stamm, Macromol. Chem. Phys. 195 (1994) 3783-3788.

[24] J.A. Elliott, S. Hanna, A.M.S. Elliott, G.E. Cooley, Macromolecules 33 (2000) 4161-4171.

[25] S. Hu, M. Lozada-Hidalgo, F.C. Wang, A. Mishchenko, F. Schedin, R.R. Nair, E.W. Hill, D.W. Boukhvalov, M.I. Katsnelson, R.A.W. Dryfe, I.V. Grigorieva, H.A. Wu, A.K. Geim, Nature, 516 (2014) 227-+.